AIAA JOURNAL
Vol. 32, No. 5, May 1994

Analytic Solutions for Dusty Shock Waves

Jack Pike*
Holly Cottage, Chawston, Bedfordshire MK44 3BH, England, United Kingdom

Exact analytical solutions are obtained for the flow of a gas carrying dust particles through a shock wave. These solutions are applicable for particular values of the dust loading ratio and heat capacity. The solutions demonstrate the types of flow which can occur and provide a series of solutions which can be used to validate numerical methods for computing dusty shock flows.

I. Introduction

THE simplest dusty shock wave flow, that of a perfect gas carrying inert particles passing through a shock wave, was considered originally by Carrier[1] and subsequently by a number of authors.[2–9] The shock wave is unaffected by the particles, but downstream of the shock a relaxation region occurs where the unchanged particle velocity and temperature behind the shock wave adjust to the new flow conditions. Even for the most basic dusty shock problem, where the particles are assumed to be spheres of constant size and gravitational forces, and particle volume and other complicating factors are neglected, the flow depends on at least six parameters, as well as relationships for the drag and heat transfer rates of the particles. The pertinent parameters for the gas flow are the freestream Mach number M_0 and the ratio of specific heats of the gas γ. The particle parameters required are the loading ratio λ, that is, the mass of dust over the mass of the gas in the freestream, and the heat capacity ratio c which is the specific heat of the dust over that of the gas. These four parameters are sufficient to find the downstream equilibrium conditions[1] when the drag and heat transfer of the particles again causes their velocity and temperature to match that of the gas. For the interaction between the particles and the gas in the relaxation region, the gas viscosity and the thermal conductivity are needed, together with the relationships for the drag and heat transfer. The flow variables can then be found as ratios to the freestream conditions at distances from the shock wave normalized in terms of a representative dust diameter and the ratio of densities.[9]

The drag and heat transfer are obtained from correlations to experimental data for spheres.[10] For the drag coefficient C_D, a close correlation to the "standard" drag curve for spheres in incompressible flow is generally used.[2–9] The heat transfer to small spheres is less well established, due to the influence of shape imperfections and surface roughness. Here, following Carrier,[1] we use the empirical relationship that for Reynolds numbers up to several thousand, the Nusselt number Nu for spheres is approximately proportional to ReC_D. At higher Reynolds numbers this relationship tends to give heat transfer rates which are too high. These correlations restrict the size of particles for which the solutions are applicable, from a minimum particle diameter d_p of a few microns, so that the gas can be treated as a continuum, to a maximum particle diameter of a few hundred microns, restricted by both the accuracy of the correlations and other assumptions such as the neglect of gravity and temperature gradients within the particle.

Even the most basic of dusty shock wave problems has needed numerical solution. This has tempted authors to include detailed estimates of the variation of the parameters within the relaxation region as well as a variety of correlations for the drag and heat transfer. These differences in the assumptions, as well as the number of parameters which need to correspond, have made it difficult to compare the solutions produced by the various numerical techniques. Some comparisons have been made[9] which indicate that discrepancies exist between the published results. Commonly, these differences might be resolved by comparison with experiment. However with experimental dusty shock waves, such is the uncertainty in the dust shape and its drag that the experimental results are used to assess the drag of the particles and are thus of limited use in validating the numerical solutions. An alternative is to compare the results with analytical solutions.

An advantage of analytical solutions is that it is relatively easy to establish that they are correct within the assumptions made, whereas with numerical solutions it is difficult to be certain that they are not subject to some programming bug or other hidden error. Hitherto complete analytic solutions for dusty shock waves have not been available. Here a set of exact analytic solutions of the basic dusty shock wave problem is found, which is both interesting in its own right and can be used to validate numerical solutions for particular values of the parameters.

II. Equations of Dusty Shock Waves

The assumptions made in developing the equations are similar to those of Carrier[1] and, in most cases, to those of subsequent authors.[2–9] The gas is assumed to obey the perfect gas equation of state, i.e.,

$$p = \rho RT \tag{1}$$

where p, ρ, and T are the gas pressure, density and temperature, respectively; and R is the gas constant. The particles are small spherical particles of equal size distributed throughout the flow, with the dominant force on the particles being the drag force, such that gravitational and other forces on the particle can be neglected. The total volume of the particles is assumed to be a negligible fraction of the gas volume, and the particles are assumed to be small enough or to have a high enough thermal conductivity such that the temperature variations within the particle can be neglected. The temperature of the particles is also assumed to be low enough for thermal radiation from the particle to be neglected.

The equations governing the flow are the conservation of mass, momentum, and energy, together with the particle drag and heat transfer equations. For one-dimensional steady flow of a dusty gas, the mass flux is constant and is given for the gas by

$$m = \rho u \tag{2}$$

and for the dust by λm. Momentum and energy conservation for the flow give[1]

$$mu + \lambda m u_p + p = \text{const} \tag{3}$$

and

$$\tfrac{1}{2} mu^2 + \tfrac{1}{2} \lambda m u_p^2 + mc_p T + \lambda mc T_p = \text{const} \tag{4}$$

Received March 20, 1993; revision received Sept. 7, 1993; accepted for publication Sept. 17, 1993.
*Member AIAA.

where u_p, T_p, and c are the velocity, temperature, and specific heat capacity of the particles, respectively, and c_p is the specific heat of the gas at constant pressure. The exchange of momentum and heat between the particles and the gas is given by the drag and heat transfer equations,[1–9] i.e.,

$$M_p \frac{du_p}{dt} = -D \tag{5}$$

$$cM_p \frac{dT_p}{dt} = hS_p(T_p - T) \tag{6}$$

where M_p is the mass of a particle, S_p is its surface area, D is the drag, and h is the coefficient of thermal conductivity. The drag and thermal conductivity are approximated by empirical fits to experimental data for spheres in terms of the nondimensional drag coefficient C_D (i.e., $D/\frac{1}{2}\rho[(u_p-u)^2A_p]$ and the Nusselt number Nu (i.e., hc_p/k, where k is the thermal conductivity of the gas). To express the equations in nondimensional form, the gas and particle variables u, u_p, T, T_p, ρ, and ρ_p are normalized in terms of their upstream values u_0, T_0, and ρ_0, respectively. The pressure is normalized with respect to $\rho_0 u_0^2$ such that the normalized pressure upstream of the shock wave p_0 is given by $1/\gamma M_0^2$. The viscosity μ of the gas is introduced via the Reynolds number Re [i.e., $\rho(u_p-u)d_p/\mu$) and the Prandtl number Pr (i.e., $\mu c_p/k$). Then Eq. (5) can be written in nondimensional form as[9]

$$\frac{du_p}{dx} = -\frac{3(u_p-u)^2 C_D}{4uu_p} \tag{7}$$

where x is the distance from the shock wave normalized by $d_p\rho_p/\rho_0$, and Eq. (6) divided by Eq. (5) becomes[1]

$$\frac{dT_p}{du_p} = \frac{\beta(T_p-T)}{c(u_p-u)} \tag{8}$$

where

$$\beta = \frac{8Nu}{PrReC_D} \tag{9}$$

With the Nusselt number approximately proportional to the Reynolds number times the drag coefficient, β may be taken as a constant. It typically has a value of order 1 as can be seen by considering the small Reynolds number limit when ReC_D has value 24 (from Stokes law) and the Nusselt number approaches its pure conduction value of 2. Then with a Prandtl number of 0.72, β has a value of 0.925. As the Reynolds number increases, ReC_D and Nu both increase so that Nu/ReC_D remains nearly constant. For smooth spheres, the variation of the Nusselt number and $ReC_D/12$ with Reynolds number is shown in Fig. 1, taken from piecewise curve fits to empirical data.[10] At larger Reynolds numbers ReC_D tends to increase faster than Nu, and the appropriate value of β is reduced.

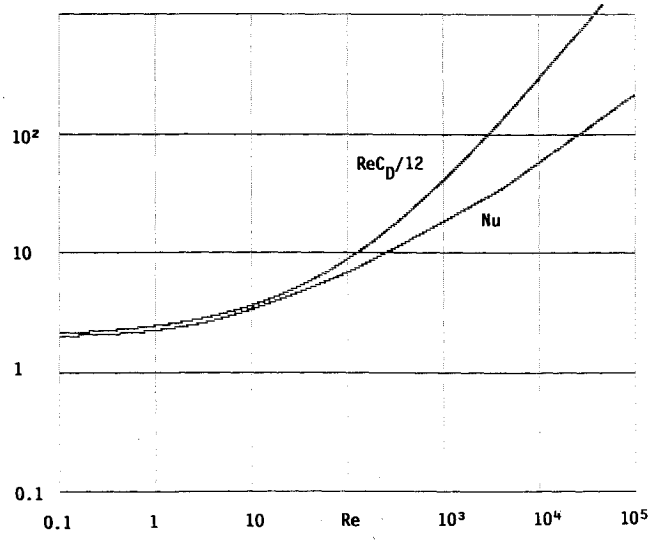

Fig. 1 Variation of Nusselt number and $ReC_D/12$ with Reynolds number for smooth spheres.

Eliminating the gas temperature from Eq. (4) using Eqs. (1–3) gives the nondimensional form of the conservation equations as[9]

$$2\gamma\lambda c p_0(T_p - 1) = (\gamma+1)U^2 - 2(1 - \gamma p_0 - \gamma\lambda U_p) - \lambda U_p[2 + (\gamma - 1)U_p] \tag{10}$$

where U_p is $1 - u_p/u_0$ and U is $1 - u/u_0$. Equation (10) expresses the dust temperature downstream of the shock wave as a quadratic function of the gas and dust velocities. Substitution of T_p from Eq. (10) in Eq. (8) gives du/du_p as a ratio of quadratics in u and u_p. Solving this equation together with Eq. (7) then gives a solution to the flow in the relaxation region. Unfortunately, this direct approach does not easily yield analytic solutions, and an alternative approach is required.

III. Analytic Solution for Dusty Shock Waves

We seek solutions where the dust velocity is a linear function of the gas velocity. We cannot be sure a priori that any such solutions exist, but if they do, then from Eq. (2) the pressure is also a linear function of the velocity and from Eqs. (1–3) and (10) the gas and dust temperatures are quadratic functions. The method used is to assume such solutions exist and to try and find combinations of the parameters for which Eqs. (7), (8), and (10) are satisfied. The linear relationship between the velocities is expressed as

$$u_p = a + bu \tag{11}$$

where a and b are constants. From conditions just downstream of the shock wave (where $u = u_1$ and $u_p = 1$) and condition at downstream equilibrium (where $u_p = u = u_e$) these constants are given by

$$a = -u_e(1 - u_1)/(u_1 - u_e) \tag{12}$$

$$b = (1 - u_e)/(u_1 - u_e) \tag{13}$$

where from Refs. 1–9 or Eqs. (1–4) the equilibrium velocity is

$$u_e = \frac{2 + 2\lambda c + (\gamma - 1)(1+\lambda)M_0^2}{(\gamma + 1 + 2\gamma\lambda c)(1+\lambda)M_0^2} \tag{14}$$

Equation (11) may also be expressed as

$$U_p = b(U - U_1) \tag{15}$$

From Eq. (10), with our linear velocity relationship, T_p can be expressed as a quadratic in U or U_p. We choose to write this relationship as

$$T_p = T + (U_p - U)(A + BU_p) \tag{16}$$

where A and B are constants that could be found from comparison of Eqs. (10) and (16). Only two constants are needed because Eq. (16) is necessarily satisfied at downstream equilibrium.

Substituting T_p from Eq. (16) into the left-hand side of Eq. (8) and integrating gives

$$T_p = 1 + \beta A U_p/c + \beta B U_p^2/2c \tag{17}$$

where the constant of integration has been fixed from conditions just downstream of the shock wave. Then for a valid solution, all

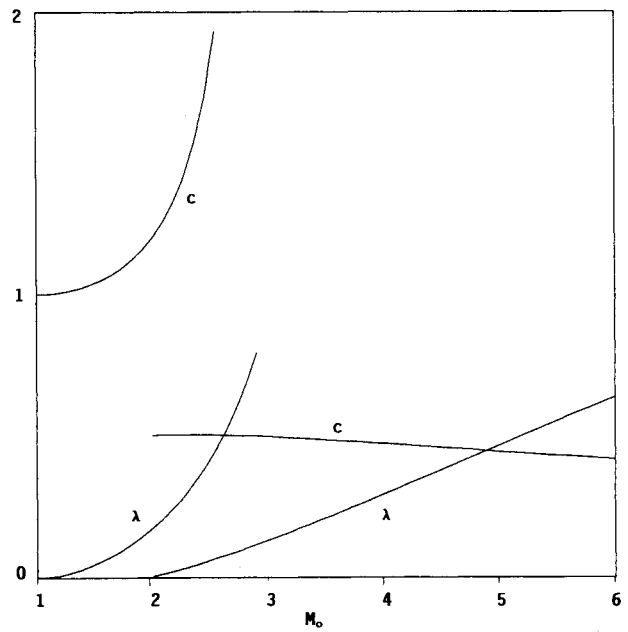

Fig. 2 Values of λ and c for analytic solution when γ = 1.2 and β = 1.

three definitions of T_p given by Eqs. (10), (16), and (17) must be identical. We assume that the values of M_0, γ, and β are given and contrive to find values of λ and c for valid analytic solutions.

Equating the constant, linear and quadratic coefficients of U_p in Eq. (17) with Eqs. (10) and (16) gives the six equations

$$A = (1 - U_1)/p_0 - 1 \tag{18}$$

$$(\gamma + 1)U_1 = 2(1 - \gamma p_0) \tag{19}$$

$$Bbp_0U_1 = Abp_0(1 - \beta/c) - 1 + (1 - U_1)(1 + \lambda b) \tag{20}$$

$$\lambda b(\gamma p_0 \beta A - \gamma U_1) = (\gamma + 1)U_1 - 1 + \gamma p_0 \tag{21}$$

$$Bbp_0(1 - b + b\beta/2c) = -(1 + \lambda b) \tag{22}$$

$$\gamma p_0 \beta \lambda bBb = \gamma + 1 + 2\gamma\lambda b - \lambda b^2(\gamma - 1) \tag{23}$$

Equation (19) gives U_1 as a function of M_0 and γ, which satisfies the conditions just downstream of the shock wave. Then Eq. (18) can be written

$$A = (\gamma - 1)(1 + \gamma M_0^2)/(\gamma + 1) \tag{24}$$

With U_1 and A known, λb can be found as a function M_0, γ, and β, from Eq. (21), i.e.,

$$\lambda b = (\gamma + 1)(M_0^2 - 1)/[\beta(\gamma - 1)(1 + \gamma M_0^2) - 2\gamma(M_0^2 - 1)] \tag{25}$$

Eliminating c from Eqs. (20) and (22) gives a linear relationship between b and Bb. This can be combined with a similar relation in Eq. (23) to give a quadratic equation in Bb, with the solution

$$Bb = \frac{-\kappa \pm \sqrt{\kappa^2 - 8\alpha(1 + \lambda b)}}{2\alpha} \tag{26}$$

where

$$\alpha = \frac{\gamma p_0^2 \beta}{\gamma - 1} - \frac{p_0 U_1}{A} \tag{27}$$

and

$$\kappa = -\frac{p_0(2\lambda b + 1 + \gamma)}{\lambda b(\gamma - 1)} - \frac{1 - (1 - U_1)(1 + \lambda b)}{A} \tag{28}$$

With λb and Bb known as functions of M_0, γ, and β, the values of λ and c may be obtained from Eqs. (23) and (22) as

$$\lambda = \frac{(\gamma - 1)(\lambda b)^2 M_0^2}{(\gamma + 1 + 2\gamma\lambda b)M_0^2 + \beta\lambda bBb} \tag{29}$$

and

$$c = \frac{\beta\lambda bBb}{2\lambda[Bb + \gamma M_0^2(1 + \lambda b)] - 2\lambda bBb} \tag{30}$$

Some values of the loading ratio and heat capacity ratio for the analytical solution to exist are listed in Table 1, for a range of Mach number, γ values of 1.2 and 1.4, and a β value of 1. Note that for $M_0 = 2.5$, two values of λ and c occur. These represent the two different solutions of the quadratic equation for Bb. The variation of λ and c with Mach number for analytic solutions is shown in Figs. 2 and 3 for γ = 1.2 and 1.4. We see that near $M_0 = 2.5$ the two solutions overlap giving analytic solutions for both large and small loading ratio at this Mach number.

Before solving the drag equation to obtain the spatial variation of the solution behind the shock wave, there is another degenerate set of solutions[9] which can be added to those given previously. If we neglect the heat capacity of the particles (i.e., put $c = 0$), then the heat transfer equation gives $T_p = T$. Using Eq. (15), Eq. (10)

Table 1 Values of λ and c for analytic solutions (β = 1)

	γ = 1.2		γ = 1.4	
M_0	λ	c	λ	c
1.5	0.047	1.038	0.065	1.058
2	0.175	1.201	0.249	1.367
2.5	0.419	1.817	0.662	5.685
2.5	0.062	0.503	0.033	0.505
3	0.132	0.496	0.101	0.506
3.5	0.210	0.485	0.170	0.501
4	0.294	0.471	0.234	0.494
4.5	0.380	0.457	0.292	0.486
5	0.467	0.443	0.345	0.479

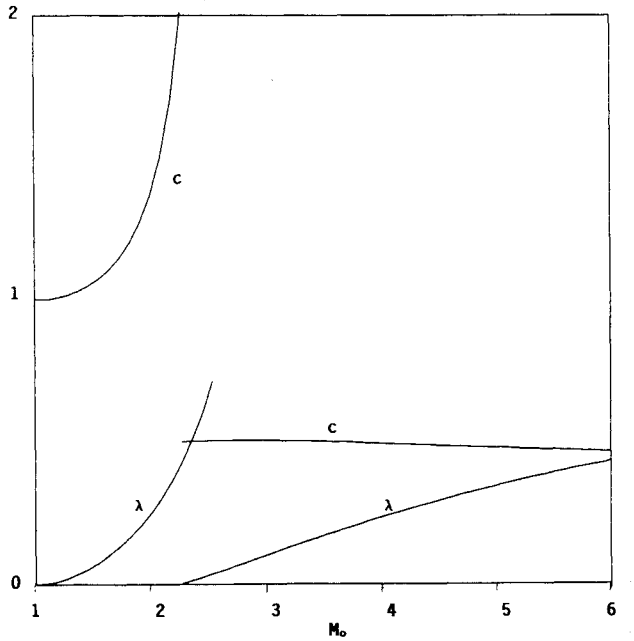

Fig. 3 Values of λ and c for analytic solution when γ = 1.4 and β = 1.

then becomes a quadratic in U which must have coefficients of value zero, giving λ as

$$\lambda = \frac{(\gamma-1)\,(M_0^2-1)^2}{M_0^2[2\gamma-(\gamma-1)M_0^2]} \tag{31}$$

This provides analytic solutions which can be used to validate numerical solutions without involving the heat transfer. Thus, if a discrepancy is found in a numerical solution, comparison with a zero heat capacity solution can help to isolate the source of the error.

These values of λ and c give solutions which have linear relationships between the velocities and pressure and quadratic forms for the temperatures. The relationship for the velocities is given by Eqs. (11–13). The linear relationship of the pressure in terms of the velocity can be obtained similarly from conditions behind the shock wave and at downstream equilibrium or from Eq. (3). The gas temperature (expressed as pu/p_0) is then given directly as a quadratic in the velocity, as is the particle temperature from Eq. (10).

IV. Solution of the Drag Equation

Analytical solution of the drag equation in the form of Eq. (7) is complicated by the occurrence of C_D. A variety of correlations for the standard sphere drag curve have been used, with the most accurate being the piecewise fit to the experimental data of Clift et al.[10] Some of the other correlations used are compared with this in Fig. 4. We see that Klyachko's correlation[11] given by

$$C_D = \frac{24}{Re}\left(1+\frac{Re^{2/3}}{6}\right) \tag{32}$$

and used in Ref. 2, agrees with Clift et al.[10] to within 5% for Reynolds numbers less than 10.[3] A correlation proposed by the present author[9] is given by

$$C_D = \frac{24}{Re}\left(1+\frac{\sqrt{Re}}{9}\right)^2 \tag{33}$$

which agrees with Clift et al.[10] to within 10% for Reynolds numbers less than 10^4. The correlation of Gilbert et al.[12] used in Refs. 3, 4, and 8 is given by

$$C_D = 0.48 + 28Re^{-0.85} \tag{34}$$

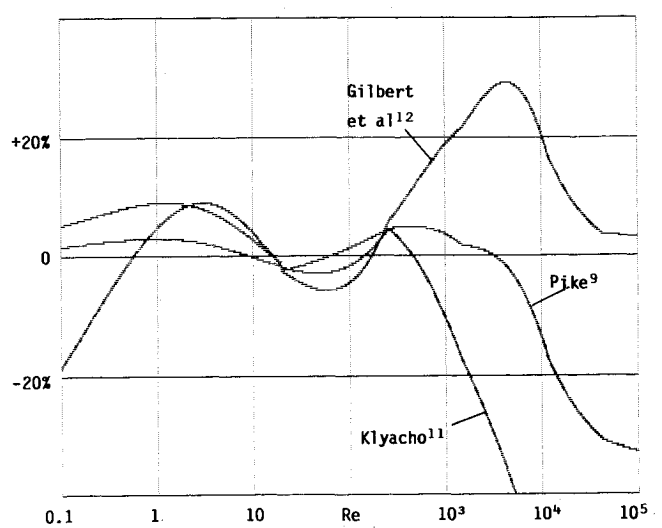

Fig. 4 Comparison of correlations for the drag of spheres.

It differs from Clift et al.[10] by up to 30% for Reynolds numbers less than 10^5. More complicated correlations have been used,[6] with a correction introduced for the variation of the drag coefficient with the Mach number of the particle, measured with respect to the flow. The effect of a difference in the correlation used on the solution can be seen from Eq. (7) to locally stretch the distance behind the shock wave by the amount of the difference. Thus, the use of Eq. (33) here will stretch the x distance by up to 10% over small regions compared with using the standard drag curve, making little difference to the solution.

The Reynolds number of the particle can be written as

$$Re = (u_p - u)/u\mu \tag{35}$$

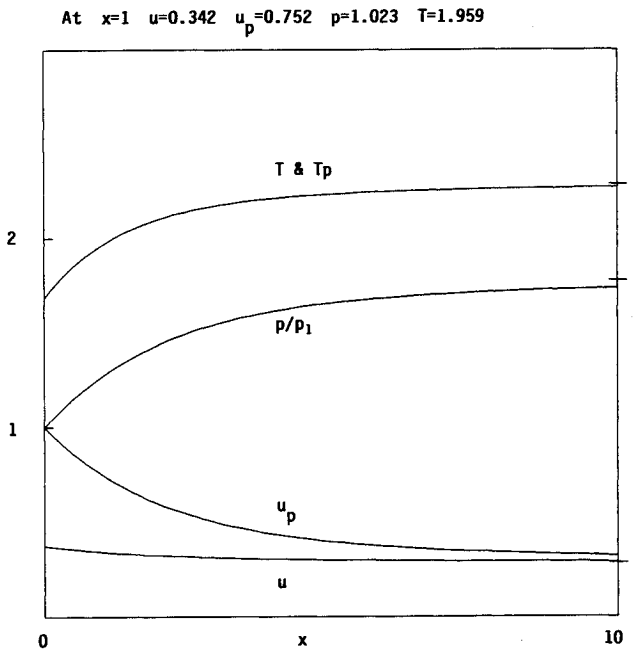

Fig. 5 Flow variation downstream of a Mach 2 shock wave for a dust with no heat capacity; $\gamma = 1.4$, $\lambda = 0.752$, and $c = 0$.

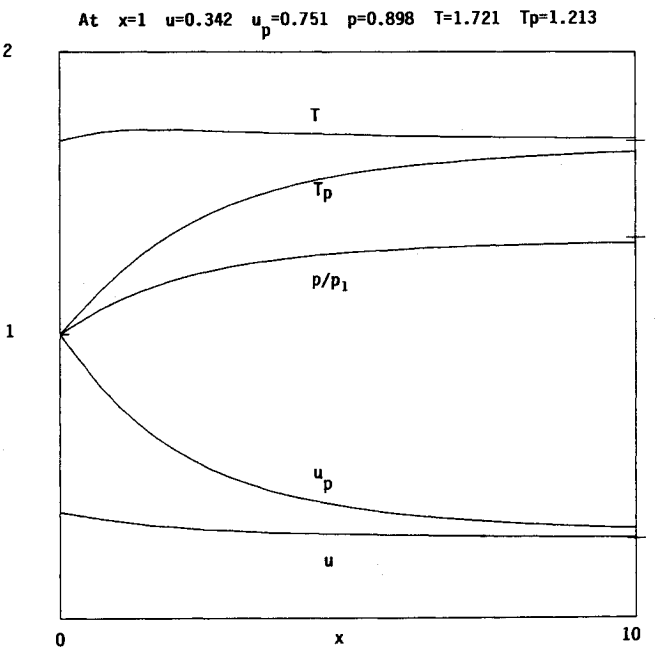

Fig. 6 Flow variation downstream of a Mach 2 shock wave for a dust with heat capacity; $\gamma = 1.4$, $\beta = 1$, $\lambda = 0.249$, $c = 1.367$, and $\mu = 4.3 \times 10^{-4}$.

where μ is the gas viscosity nondimensionalized with $\rho_0 u_0 d_p$. The viscosity is taken to be constant throughout the relaxation region. Substituting for u and u_p in Eq. (7) from Eqs. (11) and (35) gives

$$\frac{dRe}{dx} = \frac{3\mu Re^2 C_D (1 - b + \mu Re)}{4ab(1 + \mu Re)} \tag{36}$$

which after replacing C_D from Eq. (33) and simplifying becomes

$$\frac{\mu^3}{9ab}\frac{dx}{dy} = \frac{1 + \mu y^2}{(k^2 - y^2)^2 y (9 + y)^2} \tag{37}$$

where

$$y = \sqrt{Re} \tag{38}$$

and

$$k^2 = (b - 1)/\mu \tag{39}$$

The right-hand side of Eq. (37) can be expanded to give

$$\frac{\mu^3}{9ab}\frac{dx}{dy} = \frac{A_1}{k - y} + \frac{B_1}{k + y} + \frac{A_2}{(k - y)^2} + \frac{B_2}{(k + y)^2} + \frac{C_1}{y} + \frac{D_1}{9 + y} + \frac{D_2}{(9 + y)^2} \tag{40}$$

where A_1–D_2 are constants given by

$$A_2 = (1 + \mu k^2)/4k^3(9 + k)^2 \tag{41}$$

$$B_2 = (1 + \mu k^2)/4k^3(9 - k)^2 \tag{42}$$

$$D_2 = -(1 + 81\mu)/9(k^2 - 81)^2 \tag{43}$$

$$A_1 = 2A_2\{1/k(1 + \mu k^2) - 1/(9 - k)\} \tag{44}$$

$$B_1 = 2B_2\{1/k(1 + \mu k^2) + 1/(9 + k)\} \tag{45}$$

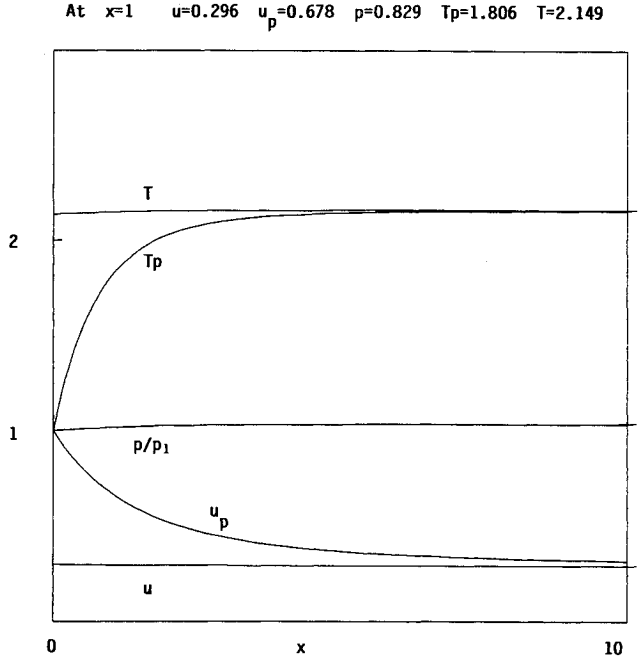

Fig. 7 Flow variation downstream of a Mach 2.5 shock wave for a dust loading ratio; $\gamma = 1.4$, $\beta = 1$, $\lambda = 0.033$, $c = 0.505$, and $\mu = 4.3 \times 10^{-4}$.

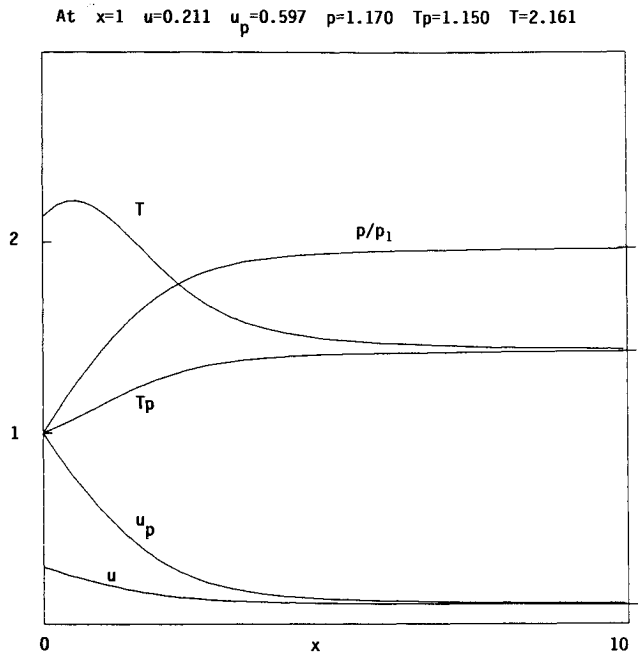

Fig. 8 Flow variation downstream of a Mach 2.5 shock wave for a dust with large heat capacity; $\gamma = 1.4$, $\beta = 1$, $\lambda = 0.662$, $c = 5.685$, and $\mu = 4.3 \times 10^{-4}$.

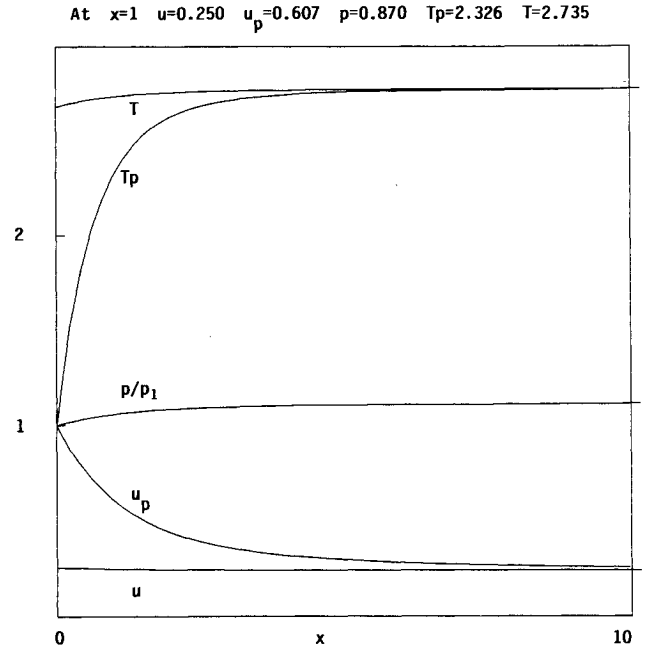

Fig. 9 Flow variation downstream of a Mach 3 shock wave for a small dust loading ratio; $\gamma = 1.4$, $\beta = 1$, $\lambda = 0.101$, $c = 0.506$, and $\mu = 4.2 \times 10^{-4}$.

$$C_1 = 1/81k^4 \tag{46}$$

$$D_1 = A_1 - B_1 - C_1 \tag{47}$$

Then integating Eq. (40) gives the distance from the shock wave as a function of the velocity. That is,

$$\mu^3 x/9ab = C_2 - A_1 \log(k - y) + B_1 \log(k + y) + A_2/(k - y) - B_2/(k + y) + C_1 \log y + D_1 \log(9 + y) - D_2/(9 + y) \tag{48}$$

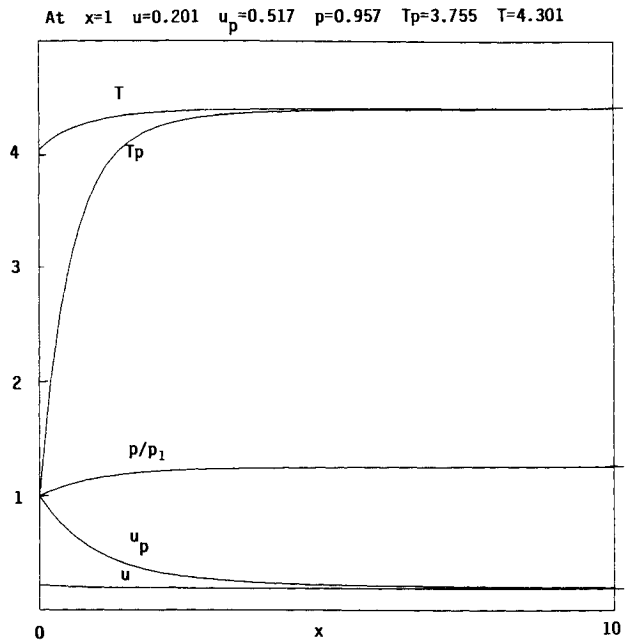

Fig. 10 Flow variation downstream of a Mach 4 shock wave for a modest dust loading ratio and heat capacity; $\gamma = 1.4$, $\beta = 1$, $\lambda = 0.234$, $c = 0.494$, and $\mu = 4.3 \times 10^{-4}$.

where C_2, the constant of integration, is obtained from conditions just downstream of the shock wave. Although Eq. (48) requires considerable algebra in its derivation, its correctness is easily checked, first by differentiating Eq. (48) to obtain Eq. (40), and then by confirming the expansion on the right- hand side of Eq. (40) by substitution of numerical values in the right-hand sides of Eqs. (37) and (40) to demonstrate that the values agree.

V. Analytic Results

In Figs. 5–10 are shown analytical solutions for Mach numbers of 2, 2.5, 3, and 4, with γ, β, and μ values of 1.4, 1, and 0.43×10^{-4}, respectively. These solutions are of different types useful for comparison and validation. On each figure the normalized flow variables (u, p, T) and the dust variables (u_p and T_p) are plotted downstream of the shock wave for x from 0 to 10. On the right-hand $x = 10$ line, tick marks indicate the asymptotic values of the flow variables far downstream (i.e., u_e, p_e/p_1, and T_e). We see that at this x value the dust and gas variables approach these limit values. To aid comparison with numerical solutions, at the top of each figure accurate values are given of the variables at $x = 1$ (i.e., a distance from the shock wave of $d_p \rho_p / \rho_0$).

The plot at $M_0 = 2$ for $\lambda = 0.75$ and $c = 0$ in Fig. 5 shows a typical flow in the relaxation region downstream of the shock wave when the heat capacity of the dust is neglected. We see that the gas pressure (plotted for convenience as p/p_1) and the temperature rise significantly behind the shock wave and that the gas and dust velocity both fall. This unexpected reduction in both velocities is needed to maintain conservation and results in the large pressure rise. Since the heat capacity of the particles is zero in this case the temperature of the gas and particles is the same.

The plot at $M_0 = 2$ in Fig. 6 shows the distribution for $\lambda = 0.249$ and $c = 1.367$. We see that the gas temperature is very nearly constant, the expected increase from the momentum exchange being reduced by the heat transferred to the dust. The pressure can be seen to rise steadily, giving a significant increase in pressure far downstream of the shock wave. The gas velocity downstream of the shock wave decreases as the dust velocity decreases to match the gas velocity.

The other plots are similar. Figure 7 shows the variation for small λ, when the changes to the gas variables behind the shock wave are small as the dust conditions seek to match the gas values. Figure 8 shows a $M = 2.5$ flow for larger values of λ and c. In this case we see that there is much greater change in the flow variables and, in particular, the gas temperature rises to a maximum and then decreases under the cooling influence of the dust to a value below T_1. Note also that the change in the pressure is nearly as large in the relaxation region as across the shock wave, and the gas velocity behind the shock wave is halved, demonstrating the significant impact the dust can have on the changes in the flow variables associated with the shock wave. Figures 9 and 10 show plots for higher Mach numbers.

VI. Conclusions

Analytical solutions of dusty shock waves for particular values of the dust loading ratio and heat capacity are found which have simple linear and quadratic relationships between the flow variables. The solutions demonstrate the types of dusty shock flows which can occur, with both the dust and gas velocities falling after the shock wave asymptotically to a downstream equilibrium value, which may be significantly less than the gas velocity behind the shock. The pressure and particle temperature both rise after the shock; and the gas temperature is shown to take various forms including rising to a maximum before falling to the downstream equilibrium temperature. An important application of the analytic solutions is to validate numerically calculated solutions to add confidence to the numerical results obtained for other types of dust.

References

[1]Carrier, G. F., "Shock Waves in a Dusty Gas," *Journal of Fluid Mechanics*, Vol. 4, 1958, pp. 376–382.

[2]Kriebel, A. R., "Analysis of Normal Shock Waves in a Particle Laden Gas," *Transactions of the ASME, Journal of Basic Engineering*, Vol. 86, Dec. 1964, pp. 655–665.

[3]Rudinger, G., and Chang, A., "Analysis of Non-Steady Two Phase Flow," *Physics of Fluids*, Vol. 7, No. 11, 1964, pp. 1747–1754.

[4]Igra, O., and Ben-Dor, G., "Dusty Shock Waves," *Applied Mechanics Reviews*, Vol. 41, No. 11, Nov. 1988, pp. 379–437.

[5]Marble, F. E., "Dynamics of Dusty Gases," *Annual Review of Fluid Mechanics*, Vol. 2, 1970, pp. 397–446.

[6]Gottlieb, J. J., and Coskunses, C. E., "Effects of Particle Volume on the Structure of a Partially Dispersed Shock Wave in a Dusty Gas," Univ. of Toronto, Rept. UTIAS 295, Toronto, Canada, Oct. 1985.

[7]Rudinger, G., "Some Properties of Shock Relaxation in Gas Flows Carrying Small Particles," *Physics of Fluids*, Vol. 7, No. 5, 1964, pp. 658–663.

[8]Muira H., and Glass, I. I., "On a Dusty Shock Tube," *Proceedings of the Royal Society, London*, Vol. A382, No. 1783, 1982, pp. 373-388.

[9]Pike, J., "Analysis of Dusty Shock Waves for a Mixed Dust," Ph.D. Thesis, College of Aeronautics, Cranfield Univ., Cranfield, England, UK, Aug. 1991.

[10]Clift, R., Grace, G. R., and Weber, M. E., *Bubbles Drops and Particles*, Academic Press, New York, 1978, p. 112.

[11]Fuchs, N. A., *The Mechanics of Aerosols*, MacMillan, New York, 1964, p. 33.

[12]Gilbert, M., Davis, L., and Altman, D., "Velocity Lag of Particles in Linearly Accelerated Combustion Gases," *Jet Propulsion Journal of the American Rocket Society*, Vol. 25, Jan. 1955, pp. 26–30.